Journal of Microbiology (2014) Vol. 52, No. 12, pp. 1036–1043
DOI 10.1007/s12275-014-4531-0

VvpM, an Extracellular Metalloprotease of *Vibrio vulnificus*, Induces Apoptotic Death of Human Cells

Mi-Ae Lee[1], Jeong-A Kim[1], Yu Jin Yang[2], Mee-Young Shin[2], Soon-Jung Park[2], and Kyu-Ho Lee[1]*

[1]*From the Department of Life Science, Sogang University, Seoul 121-742, Republic of Korea*
[2]*Department of Environmental Medical Biology, Brain Korea 21 PLUS Project for Medical Science, Yonsei University College of Medicine, Seoul 120-752, Republic of Korea*

(Received Sep 24, 2014 / Revised Oct 10, 2014 / Accepted Oct 14, 2014)

A pathogenic bacterium, *Vibrio vulnificus* produces various extracellular proteases including the elastolytic metalloprotease, VvpE. *In silico* analysis of its genome revealed a VvpE-homologous protease, VvpM whose proteolytic activity was abolished by specific inhibitors against metalloproteases. To investigate whether this newly identified protease has pathogenic role in host interaction in addition to proteolytic role, human cell lines were incubated with recombinant VvpM (rVvpM). rVvpM-challenged cells showed typical morphological changes found in cells under apoptosis. Apoptotic cell death was further evidenced by estimating the Annexin V-stained cells, whose proportions were dependent upon the concentrations of rVvpM treated to human cells. To elucidate the signaling pathway for VvpM-induced apoptosis, three MAPKs were tested if their activation were mediated by rVvpM. ERK1/2 was phosphorylated by treatment of rVvpM and rVvpM-induced cell death was blocked by a specific inhibitor against ERK1/2. In rVvpM-treated cells, the cytosolic levels of cytochrome c were increased in a VvpM concentration-dependent manner, while the levels of cytochrome c in mitochondria were decreased. Cell deaths were accompanied by apparent cleavages of procaspases-9 and -3 to the active caspases-9 and -3, respectively. Therefore, this study demonstrates that an extracellular metalloprotease of *V. vulnificus*, VvpM induces apoptosis of human cells via a pathway consisting of ERK activation, cytochrome c release, and then activation of caspases-9 and -3.

Keywords: metalloprotease, apoptosis, *Vibrio vulnificus*

Introduction

Vibrio vulnificus is a human pathogen that causes foodborne diseases including a fatal septicemia characterized by a rapid pathogenic progression and a high mortality rate (Strom and Paranjpye, 2000). Investigation of pathogenic characteristics of this pathogen has revealed that human blood cells and Jurkat T-cell lines were killed by live cells of *V. vulnificus* in a necrotic manner (Kim *et al*., 2008a, 2009). It has been further characterized that NADH oxidase-derived production of reactive oxygen species (ROS) and a subsequent ROS-dependent activation of MAPKs, p38 and ERK1/2 MAPKs are the major pathways responsible for the *V. vulnificus*-induced cell death (Kim *et al*., 2008a). In addition to occurrence of necrosis by *V. vulnificus*, live bacterial cells were able to induce apoptosis in a human macrophage cell line (Kashimoto *et al*., 2002).

Bacterial surface components such as capsular polysaccharides (Park *et al*., 2006), a lipoprotein (Goo *et al*., 2007), and lipopolysaccharides (Bahrani and Oliver, 1990), are well-known virulence factors involved in pathogenic interaction between *V. vulnificus* and host cells. Iron acquisition (Wright *et al*., 1981), fermentation efficiency (Lee *et al*., 2011), and motility (Kim and Rhee, 2003; Lee *et al*., 2004) of *V. vulnificus* are also important in its pathogenicity. In addition, extracellular proteins secreted by *V. vulnificus* are critical virulence determinants, which include a cytolytic VvhA hemolysin (Wright *et al*., 1985), a contact-dependent RtxA toxin (Lee *et al*., 2007; Kim *et al*., 2008b; Park *et al*., 2012), and an elastinolytic VvpE protease (Kothary and Kreger, 1987; Miyoshi *et al*., 1987).

Among the extracellular factors of *V. vulnificus*, an elastase VvpE, which is a 45-kDa zinc-metalloprotease belonging to the thermolysin family, has been extensively studied. Although a *vvpE*-deficient mutant *V. vulnificus* was not altered in its ability to kill mice compared with the wild type, VvpE protein itself showed to be highly cytotoxic to mice and human cells (Jeong *et al*., 2000). An injection of purified VvpE into experimental mice enhanced vascular permeability and caused hemorrhagic damage. VvpE also degrades the type IV collagen in the vascular basement membrane of human cells, leading to destruction of the basement membrane and breakdown of capillary vessels (Miyoshi *et al*., 1998). Two serine proteases sized by 59 and 53-kDa have been identified from the culture media grown by *V. vulnificus,* which are encoded by *vvsA* and *vvpS*, respectively (Wang *et al*., 2008; Lim *et al*., 2011). VvpS was shown to be an autolytic exoprotease, of which C-terminal domain has a hydrolyzing activity toward peptidoglycan. Recently, an exoprotease VvpM, which is presumed to be a zinc-metalloprotease, has been isolated from the culture supernatants of *V. vulnificus* (Lee *et al*., 2013).

The present study shows that this newly identified VvpM caused death of the human cells accompanying changes in

*For correspondence. E-mail: kyuholee@sogang.ac.kr; Tel.: +82-2-705-7963; Fax: +82-2-704-3601

cellular morphologies indicating an apoptosis. Apoptosis has been considered as one of the representative pathways for cell death, in addition to necrosis. Cell shrinkage, changes in nuclear morphology, and appearance of vacuoles in cytoplasm are the typical characteristics of apoptosis while retaining barrier function of plasma membranes. In addition, activation of apoptotic pathway involves the sequential activation of caspases (Hitomi *et al.*, 2008; Zhang *et al.*, 2009). In this study, we thus examine the effects of VvpM treatment on host cell response and death, and further define the cellular pathways responsible for the VvpM-induced cell death by monitoring key markers for apoptosis.

Materials and Methods

Cultures for bacteria and human cells

For *V. vulnificus* growth, LBS medium was prepared by addition of NaCl to LB (Bertani, 1951) at a final concentration of 2.5% (w/v) and *V. vulnificus* strains were grown at 30°C. A human colorectal carcinoma cell line, HCT-116 (10247, Korean Cell Line Bank) was grown in RPMI1640 medium (Gibco BRL, USA) supplemented with 10% heat-inactivated FBS, 2.0 mM L-glutamine, 100 U/ml penicillin G, 100 mg/ml streptomycin, 25 mM sodium bicarbonate, and 25 mM HEPES. A human colonic carcinoma cell line, HT-29 (HTB-38; American Type Culture Collection) was cultured in Dulbecco's modified Eagle's medium (DMEM; Gibco BRL) supplement with 10% fetal bovine serum (FBS), 100 U/ml penicillin G, and 100 mg/ml streptomycin. These cells were incubated at 37°C in a humid atmosphere of 5% CO_2.

Proteolysis assay of recombinant VvpM (rVvpM) secreted from *V. vulnificus*

In order to overexpress the rVvpM protein secreted from *V. vulnificus* cells, the plasmid pRK-VvpM_His_6 containing the ORF of VvpM derived from *V. vulnificus* MO6-24/O was used as previously described (Lee *et al.*, 2013). To purify rVvpM, a culture supernatant grown by *V. vulnificus* carrying pRK-VvpM_His_6 in the presence of 1.0 mM isopropyl-thio-*ß-D*-galactoside (IPTG) was subjected to Ni^+-NTA affinity chromatography (Qiagen, Germany). The presence of proteolytic activity in the purified rVvpM was examined by *in vitro* assay in a buffer (50 mM NaH_2PO_4, 300 mM NaCl, pH 8.0) including 0.5 mg/ml β-casein (33 kDa, Sigma-Aldrich, USA) as a substrate. To examine the effects of protease inhibitors on the proteolytic activity of rVvpM, 1.0 mM EDTA (Iizuka *et al.*, 1993), 1.0 mM 1,10-phenanthroline (Felber *et al.*, 1962), and 0.1 mM PMSF (Prouty and Goldberg, 1972) were added to the reaction mixtures. Resultant reaction mixtures were analyzed by SDS-PAGE.

Morphologic observation of human cell lines via transmission electron microscopy (TEM)

HCT-116 or HT-29 cells were seeded in a 24-well plate (2×10^5 cells/well) and incubated at 37°C for 24 h. At 70% confluency, prepared cells were treated with 0.1 μM rVvpM at 37°C for 6 h, and washed with pre-cooled PBS (pH 7.2). The harvested cells were fixed with 2% glutaraldehyde/2% paraformaldehyde solution at 4°C, and then embedded in paraffin. The sections of the prepared cells were observed under TEM (Philips/FEI), and the acquired images were captured using MegaView 3 camera (Olympus Soft Imaging Solutions).

Flow cytometric measurement of cell death

HCT-116 or HT-29 was seeded in a 12-well plate (5×10^5 cells/well) and incubated at 37°C for 24 h. After washing with FBS-free medium, the cells were treated with various concentrations of rVvpM (from 0.01 to 0.5 μM) at 37°C for 6 h. As a positive control for the cell death, each cell was treated with 10 mM H_2O_2 for 3 h. Cells were then stained with Annexin V (BD Pharmingen, USA) at a final concentration of 0.5 mg/ml, and the degrees of dye-binding were assessed using FACS analysis. FACS analyses were performed at least 10,000 cells per sample with a FACScan (Becton Dickinson, USA).

Western blot analysis to examine MAPK activation in rVvpM-treated cells

HCT-116 cells (2×10^5 cells/well) challenged with 0.1 or 0.5 μM of rVvpM for various lengths of time (2, 4, and 6 h) were treated in ice-cold lysis buffer [10 mM Tris-HCl, 5 mM EDTA, 130 mM NaCl, 1% (v/v) Triton X-100, 1% (v/v) PMSF, 1% (v/v) protease inhibitor, pH 7.4] for 30 min. Ten microgram of proteins in the lysate was subjected to SDS-PAGE and transferred onto a polyvinylidene fluoride membrane (Millipore Corp., USA). Membranes were blocked with 5% non-fat dry milk in TBST (Tris-buffered saline with Tween 20; 150 mM NaCl, 50 mM Tris-HCl, and 0.1% Tween 20, pH 8.0), and then incubated overnight at 4°C with antibodies specific to the phosphorylated forms of MAPK (ERK1/2, JNK, and p38 MAPK: Cell Signaling Technology, USA). After incubating with horseradish peroxidase-conjugated secondary antibodies, immunoreactive bands were visualized using an enhanced chemiluminescence system (Amersham Pharmacia Biotech, USA). Membranes were then incubated in stripping buffer (100 mM 2-mercaptoethanol, 2% SDS, and 62.5 mM Tris-HCl, pH 6.7) at 55°C for 30 min to remove the antibodies bound to phosphorylated MAPK from the membranes, and re-probed with antibodies specific to both phosphorylated and unphosphorylated forms of each MAPK.

Treatment of human cells with MAPK inhibitors prior to rVvpM exposure

To investigate the role of each MAPK in rVvpM-induced death of HCT-116 cells, the cells (4×10^4 cells/well) were treated for 30 min with 10 μM PD98059 (Calbiochem, Germany) or SB202190 (Calbiochem), which is an ERK1/2-specific inhibitor or a p38-specific inhibitor, respectively. Pretreated cells were then exposed to 0.5 μM rVvpM for 3 h. Cell viability of HCT-116 cells was measured by MTS assays using CellTiter 96® Aqueous Non-Radioactive Cell Proliferation (Promega, USA), as directed by the manual. DMSO was used to dissolve the inhibitors, and the DMSO concentrations added to cell cultures were not exceed by 1% of the culture volume, at which cellular viability of HCT-116 was not affected (data not shown).

Isolation of mitochondria and estimation of cytochrome c contents

HCT-116 was seeded in a 6-well plate (1×10^6 cells/well) and incubated at 37°C for 24 h in a 5% CO_2 incubator. After washing with FBS-free RPMI medium, the cells were treated with various concentrations of rVvpM (from 0.01 to 0.5 μM) for 6 h. Mitochondrial fraction was prepared from rVvpM-treated cells using Qproteome™ Mitochondrial Isolation Kit (Qiagen, Germany) and the contents of cytochrome c in the fraction were measured using Human Cytochrome c Quantikine ELISA Kit (R&D Systems, USA), as directed by the manuals. A standard curve for cytochrome c quantification was plotted using various amounts of human cytochrome c (R&D Systems) in the same assay. To compare cytochrome c levels in cytosolic and mitochondrial fractions, western blot analyses were performed using the monoclonal antibodies specific to human cytochrome c (Cell Signaling Technology).

Western blot analysis of caspase-9 and caspase-3

Fifty micrograms of the cell extracts treated with rVvpM were separated on 10% SDS-PAGE, and probed with anti-caspase-9 or anti-caspase-3 monoclonal antibodies (Cell Signaling Technology). A protein extract derived from cells treated with 5 μM staurosporine (STS) for 6 h was used as a positive control. A western blot of the same extracts using anti-β-actin antibodies (Cell Signaling Technology) was also done to provide a loading control.

Statistical analyses

Results were expressed as the averages ± standard deviations from at least three independent experiments. Statistical analysis for pairwise comparison was performed using Student's *t*-test (SYSTAT program, SigmaPlot version 9, Systat Software Inc.). A *p*-value <0.05 was considered statistically significant and the *p*-values are presented in the corresponding figures with single asterisk (*) for $0.01<p<0.05$ or double asterisks (**) for $p<0.01$.

Results

Identification of an additional extracellular metalloprotease produced by *V. vulnificus*

It has been previously observed that a *V. vulnificus* mutant deficient in both *vvpE* and *vvpS* genes encoding elastase and serine protease produced a certain level of exoproteolytic activity (Kim, J.-A. and Lee, K.-H., unpublished data). It

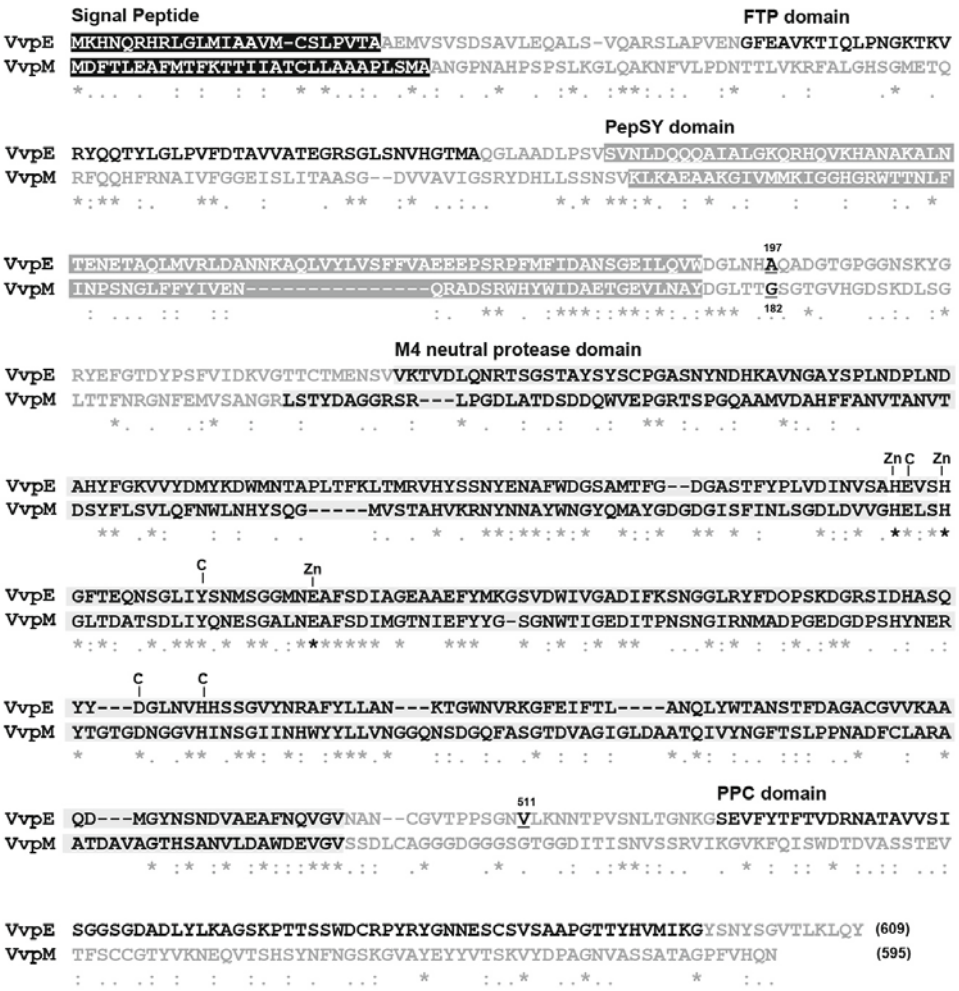

Fig. 1. Amino acid alignment of VvpM with VvpE. Both VvpE and VvpM show the presence of PepSY domain (designated by white letters in gray box) and M4 neutral protease domain (designated by black letters in gray box) that includes the conserved amino acid residues for the zinc-binding motif (marked by Zn) and for the catalytic sites (marked by C). Domains of FTP and PPC present in the N- and C-termini of VvpE are designated with black letters, and the signal peptide of VvpE was indicated by black box. The amino acid residues of N- and C-termini of the mature VvpE after the propeptides have been processed, are indicated with underlines with the amino acid positions, 197 and 511 (Miyoshi *et al.*, 1997). A putative signal peptide of VvpM (designated by black box) was predicted by the program SignalP 4.1 server and the N-terminus of the mature VvpM was identified by N-terminal sequencing, which is indicated by underlining the amino acid positioned at the 182nd residue.

suggests the presence of other exoproteases than VvpE and VvpS in the culture supernatant of *V. vulnificus*. Thus, its genome was analyzed to search the ORFs homologous to the amino acid sequences of VvpE (VVMO6_04367) or VvpS (VVMO6_01684). Among various homologous ones, at least six ORFs, VVMO6_03483, VVMO6_04535, VVMO6_01702, VVMO6_02450, VVMO6_03691, and VVMO6_04351, are shown to include tentative leader peptides at their N-termini, which were examined using the SignalP 4.1 server. VVMO6_03483, which is composed of 595 amino acids, shows an overall similarity of 56.5% to VvpE composed of 609 amino acids. Domain analysis using the NCBI Conserved Domain Search predicts that the gene product of VVMO6_03483 contains the domains of PepSY [peptidase propeptide and YPEB (a protein encoded by *Bacillus subtilis ypeB* gene)], and M4 neutral protease domain with Zn-binding sites (Häse and Finkelstein, 1993), suggesting it is a zinc-metalloprotease. Thus, it has been named by VvpM. While the domains of FTP (fungalysin/thermolysin propeptide) and PPC (prepeptidase C-terminal domain) are present in the N-terminus and C-terminus of VvpE, respectively, they are not discernible in VvpM (Fig. 1).

To examine the proteolytic characteristics of this putative metalloprotease, *V. vulnificus* carrying a broad-host-range vector pRK415 containing the His-tagged *vvpM* gene (Lee *et al*., 2013) was used to overexpress rVvpM. The size of purified rVvpM is ~55 kDa (lane 2 in Fig. 2), which is less than the calculated molecular size of the polypeptide after its 29-amino acid signal peptide is removed. N-terminal sequencing of rVvpM harvested from culture supernatant of *V. vulnificus* revealed that the N-terminal amino acid of the processed polypeptide starts from Gly at the 182nd amino acid residue of the putative VvpM ORF (Fig. 1). It suggests that the N-terminal region of VvpM polypeptide has been processed after removal of its signal peptide. However, it is not known if VvpM is further processed at the C-terminus. *In vitro* proteolytic analysis showed that rVvpM exhibits an efficient protease activity to β-casein as a substrate (Fig. 2). To investigate whether VvpM exhibits the typical proteolysis shown by metalloproteases, its proteolytic activity was examined in the presence of an ion chelator or a specific inhibitor. Proteolytic activity of rVvpM was inhibited by addition of metalloprotease inhibitors, such as EDTA (Iizuka *et al*., 1993) or 1,10-phenanthroline (Felber *et al*., 1962), but not by a specific serine protease inhibitor, such as PMSF (Prouty and Goldberg, 1972), indicating that VvpM is a metalloprotease.

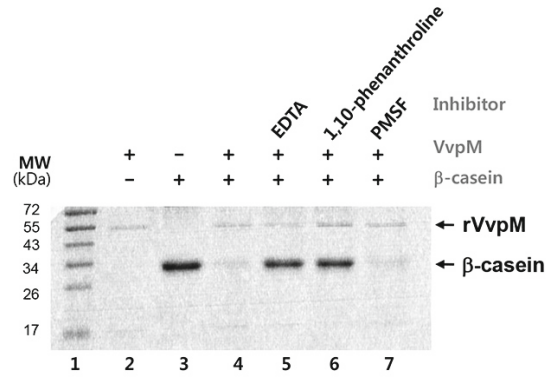

Fig. 2. ***In vitro*** **proteolytic assay using a recombinant VvpM (rVvpM).** rVvpM (0.4 μM) was incubated in a buffer including β-casein (0.5 μg/ml) as a substrate in the presence or absence of an enzyme inhibitor. Reaction mixtures were then electrophoresed on a 10% SDS-PAGE to monitor β-casein degradation. Lanes: 1, a protein size marker; 2, rVvpM only; 3, β-casein only; 4, β-casein and rVvpM; 5, β-casein, rVvpM and 1.0 mM EDTA; 6, β-casein, rVvpM and 1.0 mM 1,10-phenanthroline; and 7, β-casein, rVvpM and 0.1 mM PMSF.

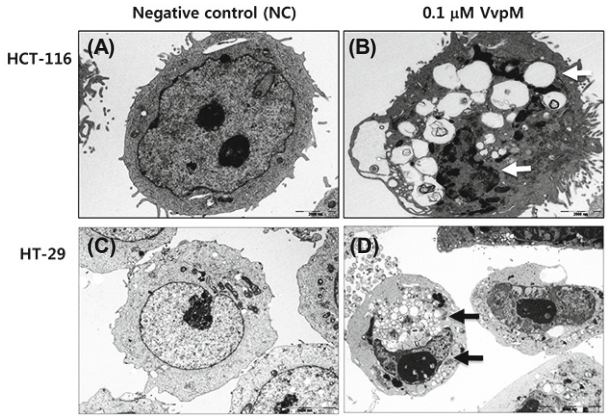

Fig. 3. Transmission electromicrographs of HCT-116 (A, B) and HT-29 cells (C, D) treated with rVvpM. HCT-116 and HT-29 cells were cultured for 6 h in the absence (A and C) or presence (B and D) of 0.1 μM rVvpM. Apparent cell shrinkage was observed in the rVvpM-treated cells accompanied by nuclear condensation and vacuole formation as indicated with arrows.

VvpM induces apoptosis in human cell lines

To investigate the functional role of VvpM, rVvpM was challenged to two human cell lines, HCT-116 and HT-29, and these two cell lines were monitored for their morphological changes. At 6 h after exposure to rVvpM (0.1 μM), both HCT-116 and HT-29 cells showed morphological changes, which have been previously described in the cells under apoptotic death (Kroemer *et al*., 2005). For example, cell shrinkage, nuclear condensation, and appearance of vacuoles were discernible in the rVvpM-treated cells (Fig. 3).

When HCT-116 cells were treated with various amounts of rVvpM (from 0.01 to 0.5 μM), the degree of Annexin V-staining was gradually increased to 36 ± 3%, while the control HCT-116 cells showed about 8% (p=0.0222, Student t-test). Increased degree of Annexin V-staining by rVvpM-treatment is comparable to the extent of Annexin V-staining of HCT-116 cells exposed to H_2O_2, a known inducer for apoptosis (Fig. 4A). When another cell line, HT-29 was exposed to rVvpM, the similar effect was also observed (Fig. 4B). About thirty percentage of cells were stained by Annexin V when HT-29 cells were challenged to 0.5 μM rVvpM (p=0.0148, Student t-test).

ERK1/2 MAPKs are involved in the VvpM-induced cell death

Three MAPK subfamilies, ERK1/2, p38, and JNK, are well-known signaling kinases involved in signal transduction in response to various extracellular stimulants including pathogenic bacterial components (Kyosseva, 2004). We thus investigated the role of MAPKs in VvpM-induced death of

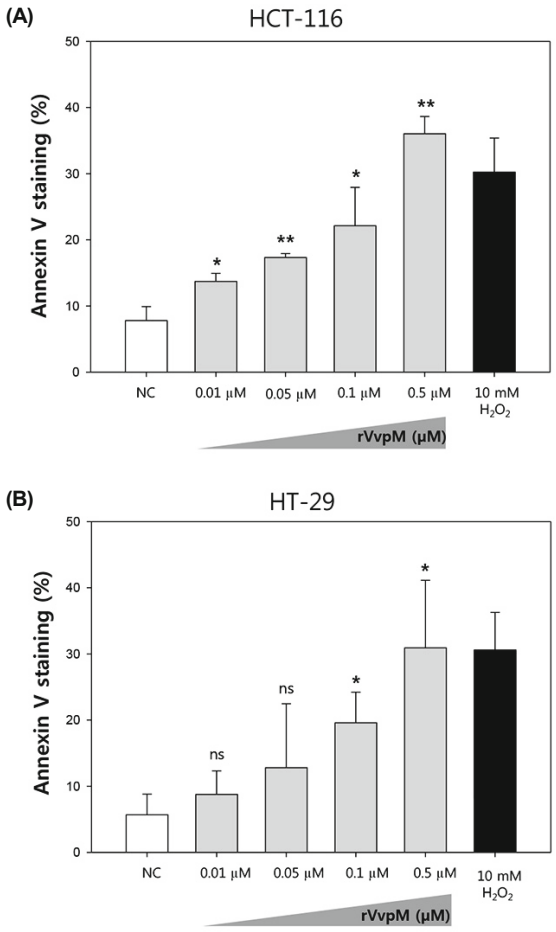

Fig. 4. Annexin V-staining of rVvpM-treated HCT-116 (A) and HT-29 cells (B). HCT-116 or HT-29 cells were treated with various concentrations of rVvpM (from 0.01 to 0.5 μM) at 37°C for 6 h. Cells were then stained with Annexin V at a final concentration of 0.5 mg/ml, and the percentages of Annexin V-stained cells were determined by FACS analysis. The cells were treated with medium only or 10 mM H_2O_2 for 3 h were served as a negative control (NC) or a positive control for cell death, respectively. Data are means ± standard deviations from three independent experiments and the *p*-values derived from comparison with the percentages of Annexin V-stained cells of NC were presented (* for $0.01<p<0.05$; ** for $p<0.01$). The term, ns, stands for non-significant difference.

HCT-116 cells by determining if incubation with rVvpM activates MAPKs in HCT-116 cells (Fig. 5A). Increase of the phosphorylated forms of p38 and ERK1/2 were apparent in HCT-116 cells treated with 0.1 or 0.5 μM rVvpM for 2 h. On the contrary, the phosphorylated form of JNK was slightly increased in only the HCT-116 cells treated with 0.5 μM rVvpM.

Role of two MAPKs, p38, and ERK1/2, in this process was assessed using a specific inhibitor against each MAPK (Fig. 5B). For this purpose, we used the MTS assay, in which viable cells could be monitored by measuring their respiratory ability to uptake MTS and comparing to that derived from the negative control (NC), in which cells were treated by DMSO. Treatment of H_2O_2 resulted in 28% of the viability relative to NC of this assay. HCT-116 cells treated with 0.5 μM rVvpM showed 74% relative viability. When HCT-116 cells were pretreated with 10 μM SB202190, a selective inhibitor of p38 MAPK, their relative viability in the presence of rVvpM was the same as the rVvpM-treated cells. On the contrary, pretreatment of HCT-116 cells with 10 μM of PD98059, a selective inhibitor of ERK1/2, resulted in abolition of rVvpM effect on the cellular viability. This result indicates that ERK1/2 MAPKs play a role in VvpM-induced death of HCT-116 cells.

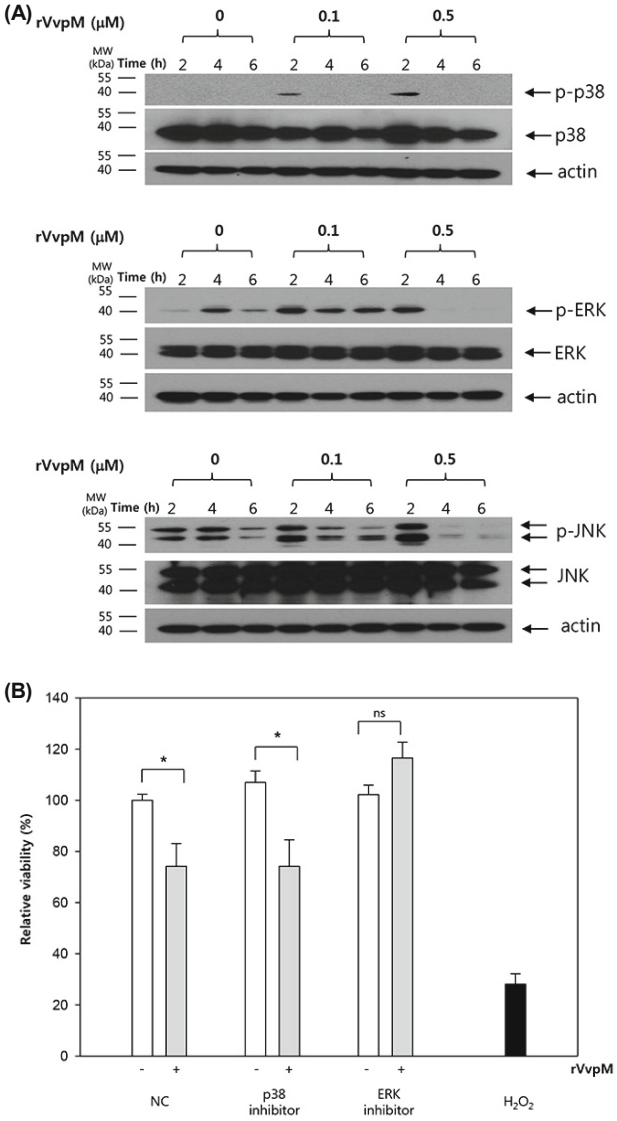

Fig. 5. Role of MAPKs in rVvpM-induced death of HCT-116. (A) Activation of MAPKs in rVvpM-treated HCT-116 cells. Lysates of HCT-116 cells challenged with 0.1 or 0.5 μM of rVvpM for 2–6 h were subjected to western blot analyses using antibodies specific to the phosphorylated form of each MAPK (ERK1/2, JNK, and p38 MAPKs). After stripping the bound antibodies, the same membranes were re-probed with antibodies specific to both phosphorylated and unphosphorylated forms of each MAPK. (B) Effects of MAPK inhibitors on rVvpM-induced death of HCT-116 cells. The cells pretreated with 10 μM PD98059 (an ERK1/2 inhibitor) or 10 μM SB202190 (a p38 inhibitor) were incubated with 0.5 μM rVvpM. After 3 h, the viability of HCT-116 cells was estimated by MTS assay, as described in Methods. Relative viability indicates the percentages of viable cells with respect to the cells treated with 1% DMSO. *p*-values were presented with single asterisk (*) for $0.01<p<0.05$ or double asterisks (**) for $p<0.01$. The term, ns, stands for non-significant difference.

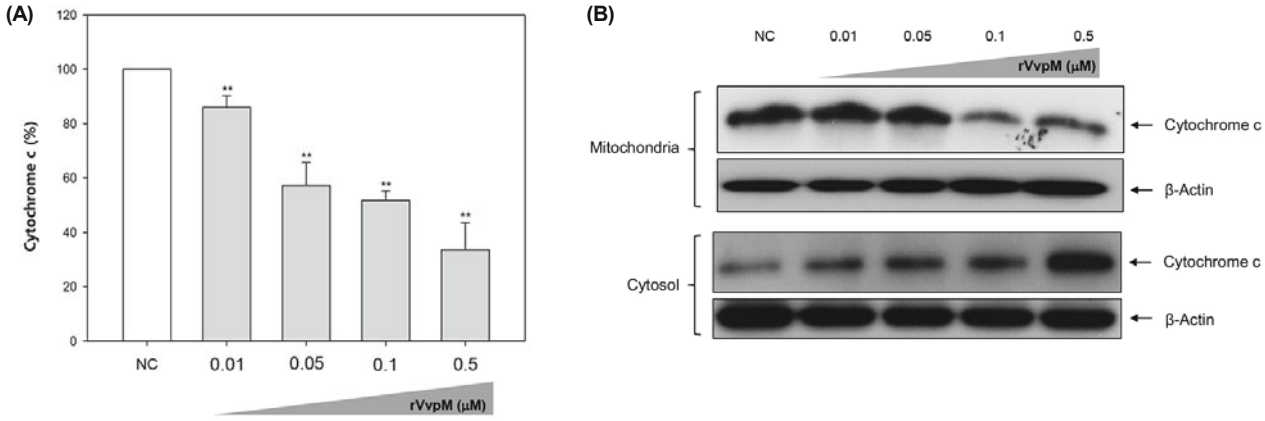

Fig. 6. Cytochrome c release from mitochondria of the rVvpM-exposed HCT-116 cells. (A) After treatment of HCT-116 cells with various concentrations of rVvpM (from 0.01 to 0.5 μM), mitochondrial fractions were assayed to quantify cytochrome c. For a negative control (NC), the cells treated with medium only were included in the assay. The percentages of cytochrome c in the mitochondrial fractions of rVvpM-treated cells, which were derived from comparison with the cytochrome c content in NC, are presented as means ± standard deviations from three independent experiments with the *p*-values (double asterisks for $p<0.01$). (B) The levels of cytochrome c in the fractions of cytosol and mitochondria of the rVvpM-treated cells were analyzed by western blotting using monoclonal antibodies specific to human cytochrome c.

VvpM induces cytochorme c release from mitochondria

Mitochondrion is one of the important components in amplifying apoptosis signal by releasing cytochrome c and other proapoptotic proteins into the cytoplasm (Green and Kroemer, 2004), resulting in formation of apoptosome with Apaf1 and procaspase-9, activation of caspases, and subsequently death of cells (Wang, 2001). Thus, it was examined whether the release of cytochrome c occurred in mitochondria of the cells challenged with rVvpM. Using mitochondrial fractions isolated from these rVvpM-treated cells, cytochrome c level was determined by ELISA. Compared to the control cells, the amounts of cytochrome c in mitochondria were significantly decreased in rVvpM-treated cells as a VvpM concentration-dependent manner (Fig. 6A; $p<0.00001$, Student *t*-test).

This finding implies that cytochrome c might be released into cytoplasm upon exposure to rVvpM. To verify the release of cytochrome c from mitochondria to cytoplasm, western blot analyses were performed with the cytoplasmic and mitochondrial fractions of rVvpM-exposed HCT-116 cells using cytochrome c-specific antibodies (Fig. 6B). Western blot of these fractions were also monitored for β-actin level as a loading control for protein amount in each samples. In untreated cells, more cytochrome c was apparent in mitochondria than in cytoplasm. When HCT-116 cells were treated with various amounts of rVvpM, the cytochrome c levels in mitochondrial fractions were decreased in a dose-dependent manner of rVvpM. In contrast, the cytochrome c levels in cytoplasmic fractions of HCT-116 cells were proportionally increased with added rVvpM. These data demonstrated that the *V. vulnificus* VvpM triggers death of HCT-116 cells via releasing cytochrome c from mitochondria of rVvpM-treated cells.

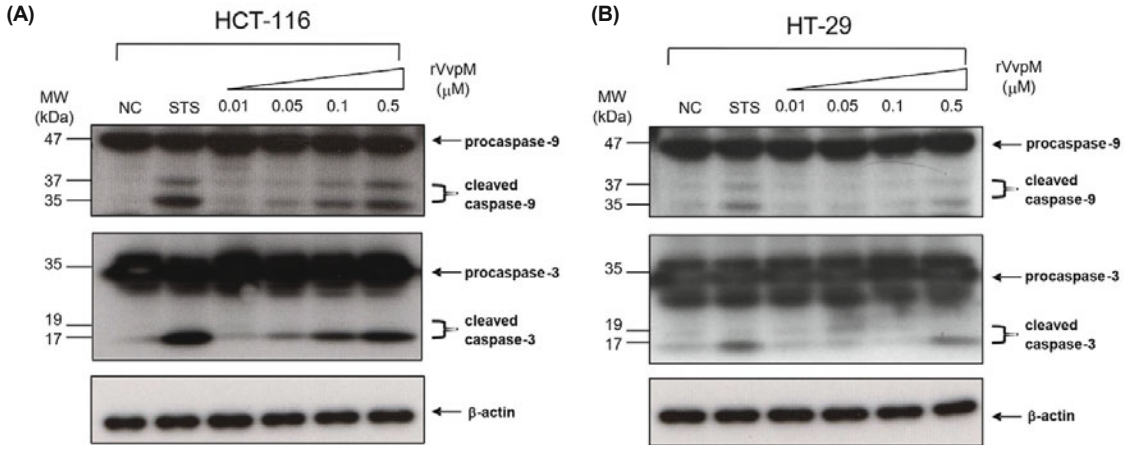

Fig. 7. Western blot analyses of caspase-3 and caspase-9 in rVvpM-exposed cell lines. Fifty microgram of the extracts of HCT-116 (A) or HT-29 cells (B) exposed to various concentrations of rVvpM (from 0.01 to 0.5 μM) were separated on 10% SDS-PAGE. The protein blots were then probed with anti-caspase-3 (the upper panels) or anti-caspase-9 (the middle panels) monoclonal antibodies. Extracts of the cells treated with medium only (NC) and 5 μM staurosporine (STS) for 6 h were included in these analyses as a negative and positive control, respectively. The level of β-actin in the same samples was monitored as a loading control (the lower panels).

VvpM activates caspases in HCT-116 and HT-29 cells

In a subsequent experiment, we performed western blotting to monitor the occurrence of caspase-9 activation in HCT-116 and HT-29 cells. Activation of caspase-3 was also examined in the same cells, since caspase-3 is a substrate for activated caspase-9 (Green, 1998). As a positive control for activation of these caspases, two human cell lines were exposed to 5 μM STS promoting activation of caspases (Bertrand *et al*., 1994). Marked activation of capsase-3 and caspase-9 were observed in STS-treated cells as expected (Fig. 7). For loading control, the same amounts of proteins in each sample were monitored by western blot analysis against β-actin. A gradual increase in proteolysis of procaspase-9 and -3 was apparent in the rVvpM-treated HCT-116 cells: the active fragments of caspase-9 and -3 were generated from the 47-kDa procaspase-9 and 35-kDa procaspase-3, respectively (Fig. 7A). The HT-29 cells, which express a mutant p53, also showed proteolyses of both procaspase-3 and procaspase-9 upon incubation with rVvpM (Fig. 7B), suggesting that rVvpM-induced apoptosis might be independent of p53. In the case of HT-29 cell, however, the caspase activation was apparent when relatively high concentration of rVvpM (0.5 μM) was challenged. These results indicate VvpM is able to induce apoptosis in both HCT-116 and HT-29 cell, which occurs in a caspase-dependent manner.

Discussion

Among diverse exoenzymes secreted by *V. vulnificus*, exoproteases have been shown to play role(s) in interactions with its hosts (Oliver *et al*., 1986; Ham and Orth, 2012). Despite of the ambiguous role of an exoproteolytic elastase, VvpE in mouse lethality of *V. vulnificus* (Jeong *et al*., 2000), VvpE has been shown to degrade human vascular basement membrane and capillary vessel, and to cause a dermonecrosis in mouse (Kothary and Kreger, 1987; Miyoshi *et al*., 1998). *In silico* analysis of *V. vulnificus* genomes showed the presence of multiple ORFs encoding proteases with the tentative but apparent signal peptides at their N-termini. A metalloprotease, VvpM was selected to investigate in this study, since VvpM shows the overall homology to the extensively studied VvpE but it does not have all the domains found in VvpE, such as FTP-domain at the N-terminus and PPC-domain at the C-terminus (Fig. 1). Thus, it was speculated that VvpM could exhibit different functions that have not been observed in VvpE. However, a proteolytic domain, M4 neutral protease domain is present in VvpM and is highly homologous to the corresponding domain of VvpE. The amino acid residues at the Zn-binding motif and the catalytic sites in this domain are conserved, and a metalloproteolytic nature of the VvpM activity was experimentally proven (Fig. 2). Both VvpE and VvpM have been shown to degrade the *V. vulnificus* hemolysin, VvhA (Lee *et al*., 2013).

Incubation of HCT-116 and HT-29 cells with rVvpM showed that this metalloprotease was able to induce death of these human cells. rVvpM-induced cell death was characterized by the typical morphological changes in cells under apoptosis, including chromatin condensation, cytoplasmic shrinkage, and membrane blebbing (Kroemer *et al*., 2005; McHugh and Turina, 2006) (Fig. 3). Some extracellular components of *Vibrio* spp. have been reported to cause apoptosis in target cells. Lipopolysaccharide of *V. fischeri* induces apoptosis in the light organs of host squid *Euprymna scolopes* for development of mutualistic interaction (Foster *et al*., 2000). A hemolysin of *V. harveyi* induces apoptosis in its putative host, *Paralichthy solivaceus* via a caspase-dependent pathway (Bai *et al*., 2010).

Monitoring of the marker proteins for apoptosis revealed that the active, cleaved forms of caspase-3 and caspase-9 were actually produced by rVvpM-treatment in a dose-dependent manner (Fig. 7). VvpM-induced activation of caspases-3/9 in an apoptotic pathway was mediated by mitochondrial release of cytochrome c (Fig. 6). The present study demonstrated that the amounts of cytochrome c was reduced in mitochondria but increased in cytosol upon exposure to VvpM, suggesting a release of cytochrome c from mitochondria in rVvpM-exposed cells. Mitochondrial dysfunction, however, has been shown to be linked to necrosis in addition to apoptosis (Kroemer *et al*., 2007). Thus, it is possible that the release of cytochrome c by VvpM could be caused by multiple types of cell death, as previously shown in other systems (Galluzzi *et al*., 2012). A previous study has reported that live bacterial cells of *V. vulnificus* induced death of human cells via activation of p38 and ERK1/2 MAPKs (Kim *et al*., 2008a, 2009). In this study, ERK1/2 was shown to be a member of signaling components for VvpM-induced cell death, based on experiments using inhibitors blocking the specific MAPK activities (Fig. 5B). These results suggest that VvpM is one of the bacterial components involved in *V. vulnificus*-induced cell death mediated by activation of the ERK1/2 MAPKs.

In the present study, we demonstrate the additional function of VvpM secreted by *V. vulnificus*, which leads apoptotic death of human cells via signaling pathway composed of activation of ERK1/2 MAPK, cytochrome c release from mitochondria, and subsequent cleavage of caspase-3 and -9. To further investigate the *in vivo* roles of VvpM in interactions of *V. vulnificus* with host(s), it is required to elucidate the specific conditions when/where *vvpM* expression is highly induced and/or VvpM activity are stably maintained.

Acknowledgements

This work was supported by the Mid-career Researcher Program through National Research Foundation (NRF) grant funded by the Ministry of Education, Science and Technology, Korea (No. 2009-0092822 to K-HL), by the Pioneer Research Center Program through NRF of Korea funded by the Ministry of Science, ICT & Future Planning (2013M3 C1A3064325) (to K-HL), and the Mid-career Researcher Program through NRF grant (No. 2010-0029116 to S-JP and S-HH).

Refernces

Bahrani, K. and Oliver, J.D. 1990. Studies on the lipopolysaccharide of virulent and avirulent strains of *Vibrio vulnificus*. *Biochem.*

Cell. Biol. **68**, 547–551.
Bai, F., Sun, B., Woo, N.Y., and Zhang, X.H. 2010. *Vibrio harveyi* hemolysin induces ultrastructural changes and apoptosis in flounder (*Paralichthy solivaceus*) cells. *Biochem. Biophys. Res. Commun.* **395**, 70–75.
Bertani, G. 1951. Studies on lysogenesis. I.: The mode of phage liberation by lysogenic *Escherichia coli*. *J. Bacteriol.* **62**, 293–300.
Bertrand, R., Solary, E., O'Connor, P., Kohn, K.W., and Pommier, Y. 1994. Induction of a common pathway of apoptosis by staurosporine. *Exp. Cell. Res.* **211**, 314–321.
Felber, J.P., Coombs, T.L., and Vallee, B.L. 1962. The mechanism of inhibition of carboxypeptidase A by 1,10-phenanthroline. *Biochemistry* **1**, 231–238.
Foster, J.S., Apicella, M.A., and McFall-Ngai, M.J. 2000. *Vibrio fischeri* lipopolysaccharide induces developmental apoptosis, but not complete morphogenesis, of the *Euprymna scolopes* symbiotic light organ. *Dev. Biol.* **226**, 242–254.
Galluzzi, L., Kepp, O., Trojel-Hansen, C., and Kroemer, G. 2012. Mitochondrial control of cellular life, stress, and death. *Circ. Res.* **111**, 1198–1207.
Goo, S.Y., Han, Y.S., Kim, W.H., Lee, K.H., and Park, S.J. 2007. *Vibrio vulnificus* IlpA-induced cytokine production is mediated by Toll-like receptor 2. *J. Biol. Chem.* **282**, 27647–27658.
Green, D.R. 1998. Apoptotic pathways: the roads to ruin. *Cell* **94**, 695–698.
Green, D.R. and Kroemer, G. 2004. The pathophysiology of mitochondrial cell death. *Science* **305**, 626–629.
Ham, H. and Orth, K. 2012. The role of type III secretion system 2 in Vibrio parahaemolyticus pathogenicity. *J. Microbiol.* **50**, 719–725.
Häse, C.C. and Finkelstein, R.A. 1993. Bacterial extracellular zinc-containing metalloproteases. *Microbiol. Rev.* **57**, 823–837.
Hitomi, J., Christofferson, D.E., Ng, A., Yao, J., Degterev, A., Xavier, R.J., and Yuan, J. 2008. Identification of a molecular signaling network that regulates a cellular necrotic cell death pathway. *Cell* **135**, 1311–1323.
Iizuka, K., Kawaguchi, H., and Kitabatake, A. 1993. Effects of thiol protease inhibitors on fodrin degradation during hypoxia in cultured myocytes. *J. Mol. Cell. Cardiol.* **25**, 1101–1109.
Jeong, K.C., Jeong, H.S., Rhee, J.H., Lee, S.E., Chung, S.S., Starks, A.M., Escudero, G.M., Gulig, P.A., and Choi, S.H. 2000. Construction and phenotypic evaluation of a *Vibrio vulnificus vvpE* mutant for elastolytic protease. *Infect. Immun.* **68**, 5096–5106.
Kashimoto, T., Ueno, S., Hanajima, M., Hayashi, H., Akeda, Y., Miyoshi, S., Hongo, T., Honda, T., and Susa, N. 2002. *Vibrio vulnificus* induces macrophage apoptosis *in vitro* and *in vivo*. *Infect. Immun.* **71**, 533–535.
Kim, W.H., Goo, S.Y., Lee, K.H., and Park, S.J. 2009. *Vibrio vulnificus*-induced cell death of human mononuclear cells requires ROS-dependent activation of p38 and ERK1/2 MAPKs. *Immunol. Invest.* **38**, 31–48.
Kim, W.H., Goo, S.Y., Shin, M.H., Chun, S.J., Lee, H., Lee, K.H., and Park S.J. 2008a. *Vibrio vulnificus*-induced death of Jurkat T-cells requires activation of p38 mitogen-activated protein kinase by NADPH oxidase-derived reactive oxygen species. *Cell. Immunol.* **253**, 81–91.
Kim, Y.R., Lee, S.E., Kook, H., Yeom, J.A., Na, H.S., Kim, S.Y., Chung, S.S., Choy, H.E., and Rhee, J.H. 2008b. *Vibrio vulnificus* RTX toxin kills host cells only after contact of the bacteria with host cells. *Cell. Microbiol.* **10**, 848–862.
Kim, Y.R. and Rhee, J.H. 2003. Flagellar basal body *flg* operon as a virulence determinant of *Vibrio vulnificus*. *Biochem. Biophys. Res. Commun.* **304**, 405–410..
Kothary, M.H. and Kreger, A.S. 1987. Purification and characterization of an elastolytic protease of *Vibrio vulnificus*. *J. Gen. Microbiol.* **133**, 1783–1791.
Kroemer, G., El-Deiry, W.W., Golstein, P., Peter, M.E., Vaux, D., Vandenabeele, P., Zhivotovsky, B., Blagosklonny, M.V., Malorni, W., Nuñez, G., and *et al.* 2005. Classification of cell death: recommendations of the nomenclature committee on cell death. *Cell Death Differ.* **12**, 1463–1467.
Kroemer, G., Galluzzi, L., and Brenner, C. 2007. Mitochondrial membrane permeabilization in cell death. *Physiol. Rev.* **87**, 99–163.
Kyosseva, S.V. 2004. Mitogen-activated protein kinase signaling. *Int. Rev. Neurobiol.* **59**, 201–220.
Lee, K.J., Jeong, C.S., An, Y.J., Lee, H.J., Park, S.J., Seok, Y.J., Kim, P., Lee, J.H., Lee, K.H., and Cha, S.S. 2011. FrsA functions as a cofactor-independent decarboxylase to control metabolic flux. *Nat. Chem. Biol.* **7**, 434–436.
Lee, J.H., Kim, M.W., Kim, B.S., Kim, S.M., Lee, B.C., Kim, T.S., and Choi, S.H. 2007. Identification and characterization of *the Vibrio vulnificus rtxA* essential for cytotoxicity *in vitro* and virulence in mice. *J. Microbiol.* **45**, 146–152.
Lee, H.J., Kim, J.A., Lee, M.A., Park, S.J., and Lee, K.H. 2013. Regulation of haemolysin (VvhA) production by ferric uptake regulator (Fur) in *Vibrio vulnificus*: repression of *vvhA* transcription by Fur and proteolysis of VvhA by Fur-repressive exoproteases. *Mol. Microbiol.* **88**, 813–826.
Lee, J., Rho, J.B., Park, K., Kim, C.B., Han, Y., Choi, S.H., Lee, K.H., and Park, S.J. 2004. Role of flagellum and motility in pathogenesis of *Vibrio vulnificus*. *Infect. Immun.* **72**, 4905–4910.
Lim, M.S., Kim, J.A., Lim, K.J., Kim, B.S., Jeong, K.C., Lee, K.H., and Choi, S.H. 2011. Identification and characterization of a novel serine protease, VvpS, that contains two functional domains and is essential for autolysis of *Vibrio vulnificus*. *J. Bacteriol.* **193**, 3722–3732.
McHugh, P. and Turina, M. 2006. Apoptosis and necrosis: a review for surgeons. *Surg. Infect. (Larchmt)* **7**, 53–68.
Miyoshi, S., Nakazawa, H., Kawata, K., Tomochika, K., Tobe, K., and Shinoda, S. 1998. Characterization of the hemorrhagic reaction caused by *Vibrio vulnificus* metalloprotease, a member of the thermolysin family. *Infect. Immun.* **66**, 4851–4855.
Miyoshi, N., Shimizu, C., Miyoshi, S., and Shinoda, S. 1987. Purification and characterization of *Vibrio vulnificus* protease. *Microbiol. Immunol.* **31**, 13–25.
Miyoshi, S., Wakae, H., Tomochika, K., and Shinoda, S. 1997. Functional domains of a zinc metalloprotease from *Vibrio vulnificus*. *J. Bacteriol.* **179**, 7606–7609.
Oliver, J.D., Wear, J.E., Thomas, M.B., Warner, M., and Linder, K. 1986. Production of extracellular enzymes and cytotoxicity by *Vibrio vulnificus*. *Diagn. Microbiol. Infect. Dis.* **5**, 99–111.
Park, J., Kim, S.M., Jeong, H.G., and Choi, S.H. 2012. Regulatory characteristics of the *Vibrio vulnificus* rtxHCA operon encoding a MARTX toxin. *J. Microbiol.* **50**, 878–881.
Park, N.Y., Lee, J.H., Kim, M.W., Jeong, H.G., Lee, B.C., Kim, T.S., and Choi, S.H. 2006. Identification of the *Vibrio vulnificus wbpP* gene and evaluation of its role in virulence. *Infect. Immun.* **74**, 721–728.
Prouty, W.F. and Goldberg, A.L. 1972. Effects of protease inhibitors on protein breakdown in *Escherichia coli*. *J. Biol. Chem.* **247**, 3341–3352.
Strom, M.S. and Paranjpye, R.N. 2000. Epidemiology and pathogenesis of *Vibrio vulnificus*. *Microb. Infect.* **2**, 177–188.
Wang, X. 2001. The expanding role of mitochondria in apoptosis. *Genes Dev.* **15**, 2922–2933.
Wang, J., Sasaki, T., Maehara, Y., Nakao, H., Tsuchiya, T., and Miyoshi, S. 2008. Variation of extracellular proteases produced by *Vibrio vulnificus* clinical isolates: Genetic diversity of the metalloprotease gene (*vvp*), and serine protease secretion by *vvp*-negative strains. *Microb. Pathog.* **44**, 494–500.
Wright, A.C., Morris, J.G. Jr., Maneval, D.R. Jr., Richardson, K., and Kaper, J.B. 1985. Cloning of the cytotoxin-hemolysin gene of *Vibrio vulnificus*. *Infect. Immun.* **50**, 922–924.
Wright, A.C., Simpson, L.M., Oliver, J.D., and Morris, J.G. Jr. 1981. Role of iron in the pathogenesis of *Vibrio vulnificus*. *Infect. Immun.* **34**, 503–507.
Zhang, D.W., Sha, J., Lin, J., Zhang, N., Lu, B.J., Lin, S.C., Dong, M.Q., and Han, J. 2009. RIP3, an energy metabolism regulator that switches TNF-induced cell death from apoptosis to necrosis. *Science* **325**, 332–336.